

# Probabilistic characteristics of narrow-band long wave run-up onshore

Sergey Gurbatov<sup>1)</sup> and Efim Pelinovsky<sup>2,3)</sup>

1) National Research University – Lobachevsky State University, Nizhny Novgorod, Russia

2) National Research University – Higher School of Economics, Moscow, Russia

3) Institute of Applied Physics, Nizhny Novgorod, Russia

## Abstract

The run-up of random long wave ensemble (swell, storm surge and tsunami) on the constant-slope beach is studied in the framework of the nonlinear shallow-water theory in the approximation of non-breaking waves. If the incident wave approaches the shore from deepest water, runup characteristics can be found in two stages: at the first stage, linear equations are solved and the wave characteristics at the fixed (undisturbed) shoreline are found, and, at the second stage, the nonlinear dynamics of the moving shoreline is studied by means of the Riemann (nonlinear) transformation of linear solutions. In the paper, detail results are obtained for quasi-harmonic (narrow-band) waves with random amplitude and phase. It is shown that the probabilistic characteristics of the runup extremes can be found from the linear theory, while the same ones of the moving shoreline - from the nonlinear theory. The role of wave breaking due to large-amplitude outliers is discussed, so that it becomes necessary to consider wave ensembles with non-Gaussian statistics within the framework of the analytical theory of non-breaking waves. The basic formulas for calculating the probabilistic characteristics of the moving shoreline and its velocity through the incident wave characteristics are given. They can be used for estimates of the flooding zone characteristics in marine natural hazards.

**Keywords:** tsunami, storm surge, long wave runup, Carrier-Greenspan transform, statistical characteristics

## 1. Introduction

The flooded area size, the water flow depth and its speed on the coast, the coastal topography characteristics ~~and the features of the coastal zone development~~ determine the consequences of marine natural disasters on the coast. The catastrophic events of recent years are well known, when tsunami waves and storm surges caused significant damage on the coast and people's death. It is worth saying that only in 2018 two catastrophic tsunamis occurred in Indonesia, leading to the death of several thousand people (on Sulawesi Island in September and in the Sunda Strait in December). The calculations of the coast flooding due to tsunamis and storm surges are mainly carried out within the framework of nonlinear shallow-water equations, taking into account the variable roughness coefficient for various areas of the coastal zone (Kaiser et al, 2011; Choi et al,

38 2012). The characteristics of the coastal destruction **is** determined either by using fragility curves  
39 (Macabuag et al, 2016; Park et al, 2017) or ~~by using a~~ direct calculation of the tsunami forces (Qi  
40 et al, 2014; Ozer et al, 2015a, b; Kian et al, 2016; Xiong et al., 2019).

41 The computation accuracy was tested on ~~a~~ series of benchmarks, including the idealized  
42 problem of the wave run-up onto the impenetrable slope of a constant gradient without friction  
43 (Synolakis et al, 2008). The nonlinear shallow water equations for the bottom geometry of this  
44 kind are linearized by using the hodograph (Legendre) transformations. This step makes it possible  
45 to obtain a number of exact solutions describing the run-up on the coast. This approach, first  
46 suggested by Carrier and Greenspan (1958), was later on used to analyze the run-up of single and  
47 periodic waves of various shapes (Synolakis, 1987; Pelinovsky and Mazova, 1992; **Carrier, 1995;**  
48 **Carrier et al, 2003;** Tinti and Toniti, 2005; Madsen and Fuhrman, 2008; Madsen and Schaffer,  
49 2010; Antuano and Brocchini, 2008, 2010; Didenkulova, 2009; Dobrokhotov et al, 2015; Aydin  
50 and Kanoglu, 2017). Moreover, such approach made it possible to determine the conditions for the  
51 wave breaking. The latter means the presence of steep fronts (gradient catastrophe) within the  
52 hyperbolic shallow water equation framework. The Carrier-Greenspan transformation was further  
53 generalized for the case of waves in an inclined channel of an arbitrary variable cross **section**  
54 (Rybkin et al, 2013; Pedersen, 2016; Shimozone, 2016; Anderson et al, 2017; Raz et al, 2018). In  
55 a number of practical cases, its use proves to be more efficient than the direct numerical  
56 computation within the 2D shallow water equation framework (Harris et al, 2015, 2016).

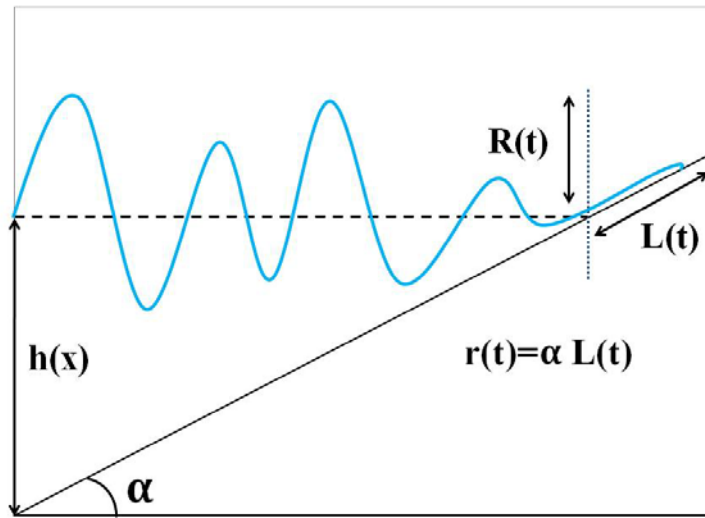
57 Due to bathymetry variability and shoreline complexity, diffraction and scattering effects lead  
58 to an irregular shape of the waves approaching the coast. Moreover, very often ~~not~~ the leading  
59 wave ~~is not turns-out-to-be~~ the maximum one. Such typical tsunami wave records on tide-gauges  
60 are well known and are not shown here. It is applied even more to swell waves, which in some  
61 cases approach the coast without breaking (Huntley et al, 1977; Hughes et al, 2010). As a result,  
62 statistical wave theory can be applied to such records and ~~with their help,~~ nonlinear shallow water  
63 equations in the random function class can be solved. This approach was used to describe the  
64 statistical moments of the long wave run-up characteristics in (Didenkulova et al, 2008, 2010,  
65 2011). Special laboratory experiments were also conducted on irregular wave run-up on a flat  
66 slope, the results of which are not very well described by theoretical dependencies (Denissenko et  
67 al, 2011, 2013). As for field data, we are acquainted with two papers: (Huntley et al, 1977; Hughes  
68 et al, 2010), where the statistical characteristics of the moving shoreline on two Canadian and one  
69 Australian beaches were calculated. They confirmed the fact that the wave process on the coast is  
70 not Gaussian. In our opinion, the main problem in the theoretical model of describing the irregular  
71 wave **run-upon** the shore is associated with the use of two hypotheses: 1) the small amplitude wave

72 field (in the linear problem) is Gaussian; 2) waves run-up on the shore without breaking. It is  
73 obvious, however, that in the nonlinear wave field some broken waves can always be present. They  
74 affect the distribution function tails and, thus, the statistical moments of the run-up characteristics  
75 as well.

76 The connection of the run-up parameters at the nonlinear stage with the linear field at a  
77 fixed point is described either in a parametric form or implicitly in a nonlinear equation  
78 (Didenkulova et al., 2010). This does not allow using the standard methods of random processes.  
79 At the same time, it is known, that this implicit equation is equivalent to a partial first-order  
80 differential equation (PDE), that is, to the simple (the Riemann wave) equation (Rudenko and  
81 Soluyan, 1977). In statistical problems, this equation arises in nonlinear acoustics. This equation  
82 or its generalization, the nonlinear diffusion equation called the Burgers equation (Burgers et al,  
83 1974) is the model equation in the hydrodynamic turbulence theory (Frisch, 1995). It should be  
84 noted that for the one-dimensional Burgers turbulence, as well as its three-dimensional version,  
85 used for the model description of the large-scale Universe structure (Gurbatov et al, 2012). It is  
86 possible to give an almost comprehensive statistical description for certain initial conditions  
87 (Gurbatov et al, 1991, 1997, 2011; Gurbatov and Saichev, 1993; Molchanov et al, 1995; Frisch,  
88 1995; Woyczynski, 1998; Frisch and Bec, 2001; Bec and Khanin, 2007). In particular, single-point  
89 and two-point probability distributions of the velocity field and even  $N$ -point probability  
90 distributions and, accordingly, multi-point moment functions were found. This partially allows  
91 using a mathematical approach developed in statistical nonlinear acoustics. An experimental study  
92 of the nonlinear evolution of random quasi-monochromatic waves and the probability distributions  
93 and spectra analysis have been carried out in acoustics more than once. They confirmed theoretical  
94 conclusions; see, for example (Gurbatov et al, 2018, 2019).

95 This paper is devoted to the analytical study of the probabilistic characteristics of the long  
96 narrow-band wave run-up on the coast. Section 2 gives the basic equations of nonlinear shallow  
97 water theory and the Carrier-Greenspan transformation, with the latter making it possible to  
98 linearize the nonlinear equations. Section 3 describes the moving shoreline dynamics when the  
99 deterministic sine wave ~~approaches~~ ~~climbs~~ the slope. The probability characteristics of the  
100 deformed sine oscillations of the moving shoreline with a random phase are described in Section  
101 4. Section 5 contains the probabilistic characteristics on the vertical displacement of the moving  
102 shoreline if the incident narrow-band wave has a random amplitude and phase. The discussion of  
103 the wave breaking effects and their influence on the distribution of the run-up characteristics is  
104 given in Section 6. The results obtained are summarized in Section 7.

105



107

108

Fig. 1. The problem geometry

109

110 Here we will consider the classical formulation of the problem of a long wave run-up on the  
 111 constant-gradient slope in an ideal fluid (Fig. 1). The wave is one-dimensional and propagates  
 112 along the  $x$ -axis directed onshore. The basin depth is a linear depth function:  $h(x) = -\alpha x$ , where  
 113  $\alpha$  is the inclination angle tangent and point  $x = 0$  corresponds to a fixed unperturbed water  
 114 shoreline.  $L(t)$  and  $r(t)$  describe the horizontal and vertical displacement of the moving shoreline,  
 115 and  $R(t)$  is the water level oscillations at  $x = 0$ . The bottom and the shore are assumed impenetrable.  
 116 The long wave dynamics is described by nonlinear shallow water equations:

$$117 \quad \frac{\partial u}{\partial t} + u \frac{\partial u}{\partial x} + g \frac{\partial \eta}{\partial x} = 0, \quad (2.1)$$

$$118 \quad \frac{\partial \eta}{\partial t} + \frac{\partial}{\partial x} [(-\alpha x + \eta)u] = 0. \quad (2.2)$$

119 Here,  $\eta(x,t)$  is the free surface elevation above the undisturbed water level, and  $u(x,t)$  is the depth-  
 120 averaged flow velocity (within the shallow water theory, the flow velocity is the same on all  
 121 horizons), and  $g$  is the gravity acceleration. Obviously, after introducing total depth

$$122 \quad H(x,t) = -\alpha x + \eta(x,t), \quad (2.3)$$

123 equations (2.1) and (2.2) are a hyperbolic system with constant coefficients. This fact makes it  
 124 possible to transform the system into a linear equation one by using a hodograph (Legendre)

125 transformation, which was done in the pioneering work (Carrier and Greenspan, 1958). As a result,  
 126 the wave field is described by a linear wave equation in the ‘cylindrical’ coordinate system

$$127 \quad \frac{\partial^2 \Phi}{\partial \lambda^2} - \frac{\partial^2 \Phi}{\partial \sigma^2} - \frac{1}{\sigma} \frac{\partial \Phi}{\partial \sigma} = 0, \quad (2.4)$$

128 and all variables are expressed in terms of an auxiliary wave function  $\Phi(\sigma, \lambda)$  using explicit  
 129 formulas

$$130 \quad \eta = \frac{1}{2g} \left( \frac{\partial \Phi}{\partial \lambda} - u^2 \right), \quad (2.5)$$

$$131 \quad u = \frac{1}{\sigma} \frac{\partial \Phi}{\partial \sigma}, \quad (2.6)$$

$$132 \quad x = \frac{1}{2\alpha g} \left( \frac{\partial \Phi}{\partial \lambda} - u^2 - \frac{\sigma^2}{2} \right), \quad (2.7)$$

$$133 \quad t = \frac{1}{\alpha g} (\lambda - u). \quad (2.8)$$

134 It should be noted that the variable  $\sigma$  is proportional to the total water depth.

$$135 \quad \sigma = 2\sqrt{gH} = 2\sqrt{g(-\alpha x + \eta)}, \quad (2.9)$$

136 so, the wave equation (2.4) is solved on the semi-axis  $\sigma \geq 0$ , and this coordinate plays the radius  
 137 role in the cylindrical coordinate system. We would like to emphasize that the point  $\sigma = 0$   
 138 corresponds to a moving shoreline, and therefore, the original problem, solved in the area with a  
 139 unknown boundary, is reduced to a fixed area problem.

140 It is important to note that the hodograph transformation is valid if the Jacobian  
 141 transformation is non-zero

$$142 \quad J = \frac{\partial(x, t)}{\partial(\sigma, \lambda)} \neq 0. \quad (2.10)$$

143 It is the case when a gradient catastrophe, identified in the framework of the shallow-water theory  
 144 with the wave breaking, does not occur. The necessary condition for the wave breaking absence is  
 145 the boundedness and smoothness of all solutions; this question will be discussed further on.

146 We will assume that the wave approaches the coast from the area far from the shoreline (  
 147  $x \rightarrow -\infty$ ), where the wave is linear. Then it is obvious that the function  $\Phi(\sigma, \lambda)$  can be completely  
 148 found from the linear theory. The difficulty in finding the wave field in the near-shoreline area is

149 due to the implicit transformation of the coordinates  $(x, t)$  to  $(\sigma, \lambda)$ . However, for the most  
 150 interesting point of the moving shoreline  $\sigma = 0$  (its dynamics determines the size of the flooded  
 151 area on the coast) all the formulas become explicit. In particular, from (2.5) and (2.6) follows

$$152 \quad r(t) = R \left[ t + \frac{u(t)}{\alpha g} \right] - \frac{u(t)^2}{2g}, \quad (2.11)$$

$$153 \quad u(t) = U \left[ t + \frac{u(t)}{\alpha g} \right], \quad (2.12)$$

154 where  $r(t)$  and  $u(t)$  are the vertical displacement of the moving shoreline and its speed, and the  
 155 functions  $R(t)$  and  $U(t)$  determine the field characteristics at the fixed point  $(x = 0)$  from the linear  
 156 theory

$$157 \quad R(t) = \frac{1}{2g} \frac{\partial \Phi(\sigma = 0, \lambda)}{\partial \lambda} \Big|_{\lambda = \alpha g t}, \quad U(t) = \frac{1}{\sigma} \frac{\partial \Phi(\sigma, \lambda)}{\partial \sigma} \Big|_{\sigma = 0, \lambda = \alpha g t}. \quad (2.13)$$

158 Then we add the obvious kinematic relations for the vertical displacement and velocity of the last  
 159 sea point along the slope.

$$160 \quad u(t) = \frac{1}{\alpha} \frac{dr(t)}{dt}, \quad U(t) = \frac{1}{\alpha} \frac{dR(t)}{dt}. \quad (2.14)$$

161 Let us note that formula (2.12) is identical to the so-called Riemann wave or a simple wave  
 162 in a nonlinear non-dispersive medium (in particular, in nonlinear acoustics), if we consider the  
 163 parameter  $1/\alpha g$  to be a ‘coordinate’; see, for example, (Rudenko and Soluyan, 1977, Gurbatov et  
 164 al, 1991, 2011). Moreover, formula (2.13) describes the integral over the Riemann wave. This  
 165 analogy proves to be very useful when transferring the already known results in the wave nonlinear  
 166 theory to the run-up characteristics described by the formulas (2.11) and (2.12) ~~ODE~~.

167 Detailed calculations of the long wave run-up on the coast were carried out repeatedly; see,  
 168 for example (Carrier and Greenspan, 1958; Synolakis, 1987; Pelinovsky and Mazova, 1992; Tinti  
 169 and Toniti, 2005; Madsen and Fuhrman, 2008; Madsen and Schaffer, 2010; Antuano and  
 170 Brocchini, 2008, 2010; Didenkulova, 2009; Dobrokhotov et al, 2015; Aydin and Kanoglu, 2017).

171 It is worth mentioning that the nonlinear time transformation in (2.11) and (2.12) leads to  
 172 the shoreline oscillation distortion in comparison with the linear theory predictions. So, for large  
 173 amplitudes the wave shape becomes multi-valued (broken). The first moment of the wave breaking  
 174 on the shoreline (the gradient catastrophe) is easily found from (2.12) by calculating the first  
 175 derivative of the moving shoreline velocity

176 
$$\frac{du}{dt} = \frac{dU/dt}{1 - \frac{dU/dt}{\alpha g}}, \quad (2.15)$$

177 from it follows the wave breaking condition

178 
$$Br = \frac{\max(dU/dt)}{\alpha g} = \frac{\max(d^2R/dt^2)}{\alpha^2 g} = 1, \quad (2.16)$$

179 where we have introduced the breaking parameter  $Br$  to designate the left-hand side in (2.16),  
 180 which characterizes the nonlinear wave properties on the shoreline. The condition (2.16) can be  
 181 given a physical meaning, that the breaking occurs when the last sea particle acceleration ( $\alpha^{-1}d^2R/dt^2$ )  
 182 exceeds the component of gravity acceleration along the shoreline ( $g\alpha$ ). As shown  
 183 in (Didenkulova, 2009), condition (2.16) coincides with (2.10) for Jacobian. It is important to  
 184 emphasize that the breaking condition is unequivocally found through solving the linear problem  
 185 of the wave run-up on the shore. It is determined only by the particle acceleration value on the  
 186 shoreline; but it is not determined separately by the shoreline displacement or its velocity.

187 A similar Carrier – Greenspan transformation is obtained for waves in narrow inclined  
 188 channels, fjords, and bays (Rybkin et al, 2013; Pedersen, 2016; Anderson et al, 2017; Raz et al,  
 189 2018); only the wave equation (2.4) and relations (2.5) - (2.8) change. However, the moving  
 190 shoreline dynamics is still described by equations (2.11) and (2.12), valid for arbitrary cross-  
 191 section channels.

192

193 **3. The moving shoreline dynamics at an initially monochromatic wave run-up**

194 The monochromatic wave run-up on a flat slope by using the Carrier – Greenspan  
 195 transformation has been studied in a number of papers cited above. Let us reproduce here the main  
 196 features of the moving shoreline dynamics necessary for us to draw the statistical description  
 197 further on. Mathematically, the monochromatic wave run-up is described by an elementary  
 198 solution of equation (2.4)

199 
$$\Phi(\sigma, \lambda) = QJ_0(l\sigma) \cos(l\lambda), \quad (3.1)$$

200 where  $Q$  and  $l$  are arbitrary constants, and  $J_0$  is the zero-order Bessel function. Far from the  
 201 shoreline ( $\sigma \rightarrow \infty$ ) the Bessel function decreases, so the wave function  $\Phi$  becomes small. In this  
 202 case, in (2.5) - (2.8) one can use approximate expressions (the ‘linear’ Carrier – Greenspan  
 203 transformation)

204 
$$\eta = \frac{1}{2g} \frac{\partial \Phi}{\partial \lambda}, \quad u = \frac{1}{\sigma} \frac{\partial \Phi}{\partial \sigma}, \quad x = -\frac{\sigma^2}{4\alpha g}, \quad t = \frac{\lambda}{\alpha g}, \quad (3.2)$$

205 and using the asymptotic representation for the Bessel function, reduce (3.1) to the expression for  
 206 the water surface displacement

207 
$$\eta(x, t) = a(x) \left\{ \sin \left[ \omega \left( t - \int \frac{dx}{\sqrt{gh(x)}} \right) \right] - \frac{\pi}{4} \right\} + \sin \left[ \omega \left( t + \int \frac{dx}{\sqrt{gh(x)}} \right) + \frac{\pi}{4} \right], \quad (3.3)$$

208 where

209 
$$a(x) = \frac{Q}{2g} \sqrt{\frac{l}{\pi \sqrt{gh(x)}}}, \quad \omega = gl\alpha. \quad (3.4)$$

210 The wave field away from the shoreline is a superposition of two waves of the same frequency  
 211 and a variable amplitude  $a(x)$ , which together form a standing wave. It immediately shows that  
 212 the wave amplitude varies with depth according to the Green law ( $h^{-1/4}$ ), as it should be far from  
 213 the coast. The same asymptotic result follows from the exact solution of linear shallow water  
 214 equations.

215 
$$\eta(x, t) = R_0 J_0 \left( \sqrt{\frac{4\omega^2 |x|}{g\alpha}} \right) \sin(\omega t), \quad (3.5)$$

216 where  $R_0$  is the wave amplitude at the fixed shoreline ( $x = 0$ ), identified with the maximum run-  
 217 up height in the linear theory. By connecting (3.4) and (3.5), we obtain the formula for the run-up  
 218 height obtained through the incident wave amplitude far from the coast

219 
$$\frac{R_0}{a(x)} = \sqrt{\frac{2\omega}{\alpha}} \sqrt{\frac{h(x)}{g}}. \quad (3.6)$$

220 Formula (3.6) allows working further with the run-up height  $R_0$  instead of the wave amplitude far  
 221 from the coast  $a(x)$ , ~~considering it to be given. This run-up height will be considered as the given~~  
 222 ~~value.~~ Having determined  $Q$  and  $l$  through the incident wave parameters, we can calculate the run-  
 223 up characteristics in the nonlinear theory, considering the limit of formula (3.1) with  $\sigma \rightarrow 0$  and  
 224 using the Carrier – Greenspan transformation formulas (2.5) - (2.8). The moving shoreline  
 225 movement is determined by the parametric dependence

226 
$$t = \frac{\lambda}{\alpha g} - \frac{\omega R_0}{\alpha^2 g} \cos \left( \frac{\omega \lambda}{\alpha g} \right), \quad (3.7)$$

227 
$$r = R_0 \sin \left( \frac{\omega \lambda}{\alpha g} \right) - \frac{\omega^2 R_0^2}{2\alpha^2 g} \cos^2 \left( \frac{\omega \lambda}{\alpha g} \right). \quad (3.8)$$



228 It is convenient to introduce dimensionless variables

$$229 \quad z = \frac{r}{R_0}, \quad \tau = \omega t, \quad \varphi = \frac{\omega \lambda}{\alpha g}, \quad (3.9)$$

230 and calculate the breaking parameter

$$231 \quad Br = \frac{\omega^2 R_0}{\alpha^2 g}, \quad (3.10)$$

232 so the formulas (3.7) and (3.8) are finally rewritten in the form

$$233 \quad \tau = \varphi - Br \cos(\varphi), \quad (3.11)$$

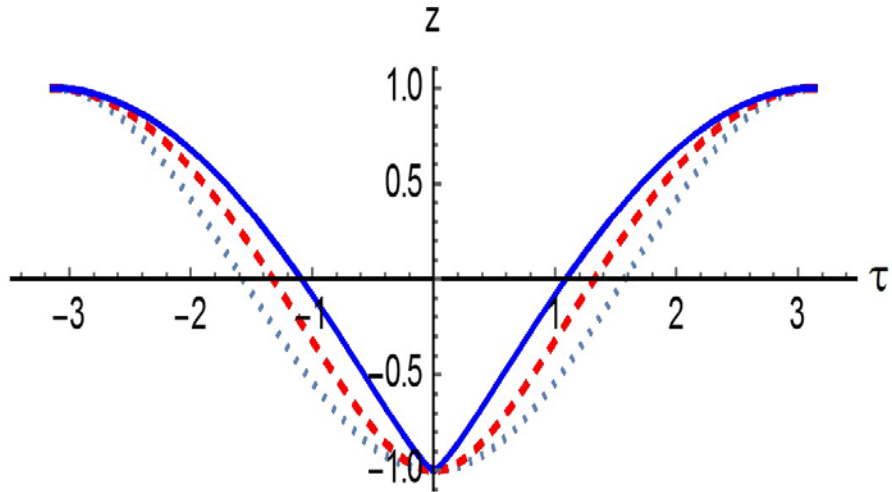
$$234 \quad z = \sin(\varphi) - \frac{Br}{2} \cos^2(\varphi), \quad (3.12)$$

235 what is another ~~expression record~~ expression for the formulas (2.11) and (2.12), if we take

$$236 \quad R(t) = R_0 \sin(\omega t), \quad (3.13)$$

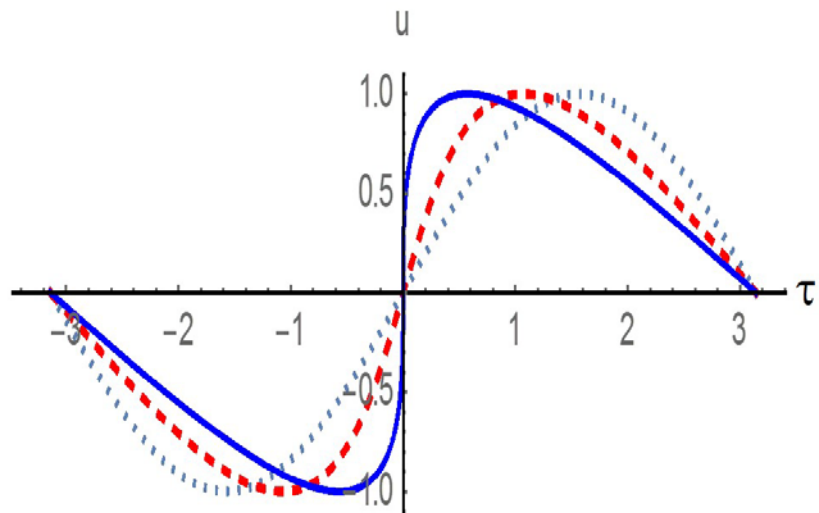
237 arising from (3.5) with  $x = 0$ . Let us note that the function  $z(\tau, Br)$  is set in a parametric form, but  
238 after expressing  $\varphi$  from (3.12) and substituting it in (3.11), we can obtain the explicit expression  
239 for the function  $\tau(z; Br)$ . In the paper, we will use both explicit and implicit expressions of the  
240 functions describing the moving shoreline dynamics.

241 Fig. 2 shows the moving shoreline dynamics at different wave height values in terms of the  
242 breaking parameter up to the limiting value ( $Br = 1$ ). In the limit of small parameter values, the  
243 oscillations are close to sinusoidal (it is almost a linear problem). Then, with the increasing  
244 amplitude, the moving shoreline velocity gets a steep leading front, while at the moving shoreline  
245 vertical displacement a peculiar feature is formed at the wave run-down stage. As it is known, at  
246 the time of the Riemann wave breaking, a peculiarity like  $u \sim t^{1/3}$  is formed (Pelinovsky et al,  
247 2013). Then, in the integral over the Riemann wave (at the moving shoreline displacement), this  
248 peculiar feature will have the form  $z \sim t^{4/3}$ . Thus, with the wave amplitude increase, the first  
249 breaking occurs at sea (at the run-down stage), and not on the coast. Then the breaking zone  
250 expands and moves on to the coast, but at this stage, analytical solutions based on the Carrier-  
251 Greenspan transformation become inapplicable.



252

253



254

255

256 Fig. 2. The moving shoreline dynamics (top) and its velocity (below) in the case of the incident  
 257 monochromatic wave for different breaking parameter values  $Br$  (0 – the dotted line, 0.5 – the  
 258 dashed line and 1 – the solid line).

259

260

#### 4. Probabilistic characteristics of the initially sine wave run-up with a random phase

261

262

263

264

Let us now consider the probabilistic characteristics of the initially sine wave run-up with a random phase on the shore, assuming it to be uniformly distributed over the interval  $[0 - 2\pi]$ . These characteristics are found by using the geometric probability methods (Kendall and Stuart, 1969), so that for ergodic processes the probability density of the moving shoreline vertical

265 displacement coincides with the relative location time of the function  $z(\tau)$  in the interval  $(z,$   
 266  $z + dz)$

$$267 \quad W(z) = \frac{1}{2\pi} \sum_{n=1}^N \left| \frac{d\tau_n}{dz} \right|, \quad (4.1)$$

268 where the summation takes place at all intersection levels  $z(\tau)$ . For harmonic disturbance, it is  
 269 enough to restrict ourselves to considering the field on a half-period. So, for the moving shoreline  
 270 vertical displacement in dimensionless variables, the derivative  $d\tau/dz$  of the parametric curve  
 271 (3.11) and (3.12) can be calculated through the ratio of the derivatives  $d\tau/d\varphi$  and  $dz/d\varphi$

$$272 \quad W_z^{\sin}(z; Br) = \frac{1}{\pi} \frac{1 + Br \sin \varphi}{\cos \varphi + Br \cos \varphi \sin \varphi} = \frac{1}{\pi \cos \varphi}, \quad (4.2)$$

273 we indicated here that the probability density depends on  $Br$  as a parameter. Finding  $\cos \varphi$  from  
 274 the formula (3.12) for the vertical displacement, we obtain the final expression for the probability  
 275 density

$$276 \quad W_z^{\sin}(z; Br) = \frac{1}{\pi} \frac{1}{\sqrt{1 - \frac{1}{Br^2} \left[ 1 - \sqrt{1 + 2zBr + Br^2} \right]^2}}, \quad (4.3)$$

277 which in the linear problem for a purely sinusoidal perturbation transforms into a well-known  
 278 expression for the probability distribution of a harmonic signal with a random phase (Kendall and  
 279 Stuart, 1969)

$$280 \quad W_z^{\sin}(z; 0) = \frac{1}{\pi} \frac{1}{\sqrt{1 - z^2}}. \quad (4.4)$$

281 The probability distribution (4.3) for the three values of the parameter  $Br$  is shown in Fig.3.  
 282 As you can see, the probability density becomes an asymmetric function with a greater probability  
 283 in the area of positive values corresponding to the wave run-up on the coast than at the run-down  
 284 stage. At the ends of the interval, the probability density is unlimited throughout the entire range  
 285 change of  $Br$ , since the shoreline oscillations near the maximum have a zero derivative (the moving  
 286 shoreline velocity in it becomes zero).

287 The obtained probability density function can be used to calculate the statistical moments  
 288 of the shoreline oscillations. Technically, however, it is easier to use the parametric equations  
 289 (3.11) and (3.12) and calculate all the moments.

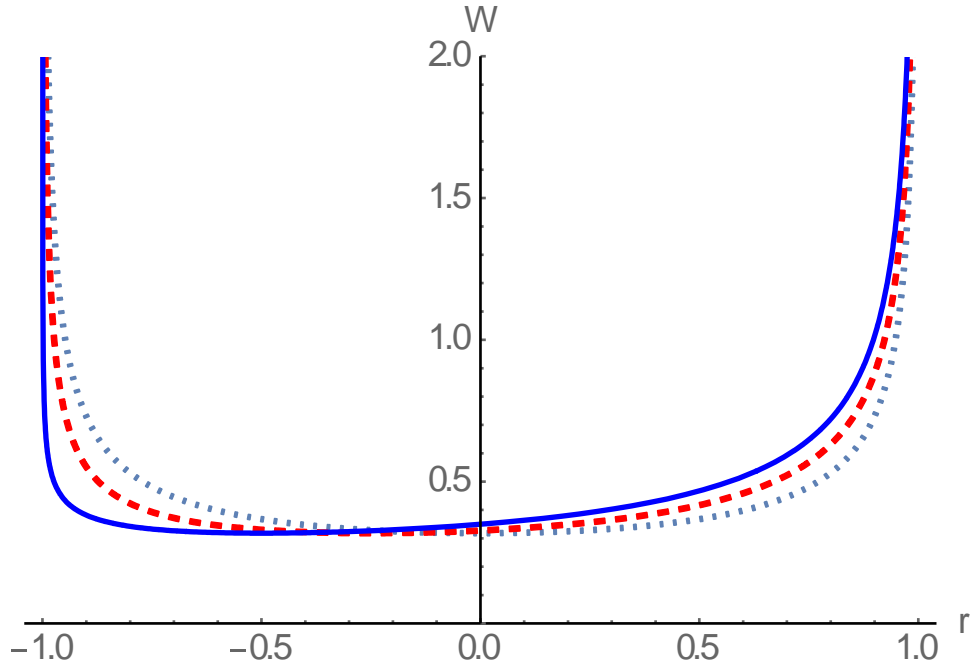
$$290 \quad M_n^z = \frac{1}{2\pi} \int_0^{2\pi} z^n(\tau) d\tau = \frac{1}{2\pi} \int_0^{2\pi} z^n(\varphi) \frac{d\tau}{d\varphi} d\varphi. \quad (4.5)$$

291 So, the first moment

$$292 \quad M_1^z = \frac{Br}{4} \quad (4.6)$$

293 determines the average water level rise on the coast when the waves approach the shore (set-up  
294 phenomenon), which is commonly observed (Dean and Walton, 2009).

295



296

297 Fig. 3. The probability density of the moving shoreline vertical displacement for the initially sine  
298 wave run-up at  $Br = 0$  (the dotted line),  $0.5$  (the dashed line) and  $1$  (the solid line).

299

300 The second moment determines the dispersion

$$301 \quad \delta^2 = \frac{1}{2\pi} \int_0^{2\pi} (z - M_1^z)^2 d\tau = \frac{1}{2} - \frac{3}{32} Br^2, \quad (4.7)$$

302 characterizing the fluctuation range relative to the average value; it relatively weakly decreases  
303 with the growth of the parameter  $Br$  (less than 10% for non-breaking waves).

304 Finally, the total flooding time and its drainage time are easy to find from (3.11) and (3.12),  
305 finding from the equation (3.12) mentioned last, the value  $\varphi$ , at which  $z = 0$ , and substituting the  
306 obtained values in (3.11)

$$307 \quad T_{flood} = \pi - 2 \arcsin \left[ \frac{\sqrt{1 + Br^2} - 1}{Br} \right] + 2\sqrt{2} \sqrt{\sqrt{1 + Br^2} - 1}, \quad (4.9)$$

308

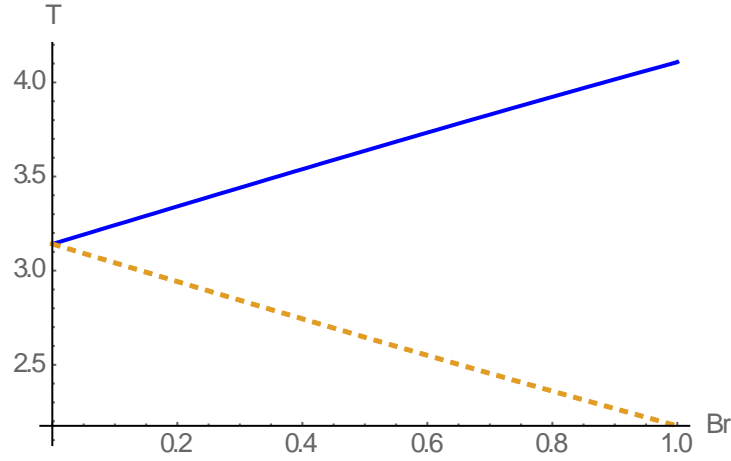
309

$$T_{dry} = \pi + 2 \arcsin \left[ \frac{\sqrt{1 + Br^2} - 1}{Br} \right] - 2\sqrt{2}\sqrt{\sqrt{1 + Br^2} - 1},$$

310

Both times change almost linearly with the increasing wave amplitude (parameter  $Br$ ), see Fig. 4.

311



312

Fig. 4. The total flooding time (the solid curve) and the drainage time (the dashed curve) depending on the parameter  $Br$ .

314

315

It is worth noting that, in contrast to the vertical displacement, the moving shoreline velocity distribution  $[u = (\omega R_0 / \alpha)v]$ , as it is easy to show, does not depend on the breaking parameter and probability density function is determined by the simple formula

318

$$W_v^{\sin}(v) = \frac{1}{\pi} \frac{1}{\sqrt{1-v^2}}. \quad (4.10)$$

319

The distribution independence on the degree of nonlinearity is well known for the Riemann waves and is explained by the compensation of compression and rarefaction areas (Gurbatov et al, 1991, 2011).

322

323

324

### 5. Probabilistic characteristics of a narrow-band wave run-up with a random amplitude and phase

325

Let us consider the run-up of a quasi-harmonic wave with a random amplitude and phase on a flat slope. To do this, we will first rewrite formulas (4.3) and (4.10) for them to include the wave amplitude. It is convenient to enter the maximum height  $R_{max}$  as the amplitude scales at which the breaking parameter turns into 1

329

$$Br = \frac{\omega^2 R_{max}}{\alpha^2 g} = 1, \quad (5.1)$$

330 and to use dimensionless displacement ( $y=r/R_{max}$ ). Then the dimensionless amplitude is

$$331 \quad A = \frac{R_0}{R_{max}} \leq 1, \quad (5.2)$$

332 and formula (4.3) is converted to the form ( $-A < y < A$ )

$$333 \quad W_y^{\sin}(y; A) = \frac{1}{\pi} \frac{1}{\sqrt{A^2 - \left[1 - \sqrt{1 + 2y + A^2}\right]^2}}. \quad (5.3)$$

334 Assuming now that the wave amplitude  $A$  is a random variable, we average (5.3) by using  
335 the amplitude distribution density  $W_A(A)$

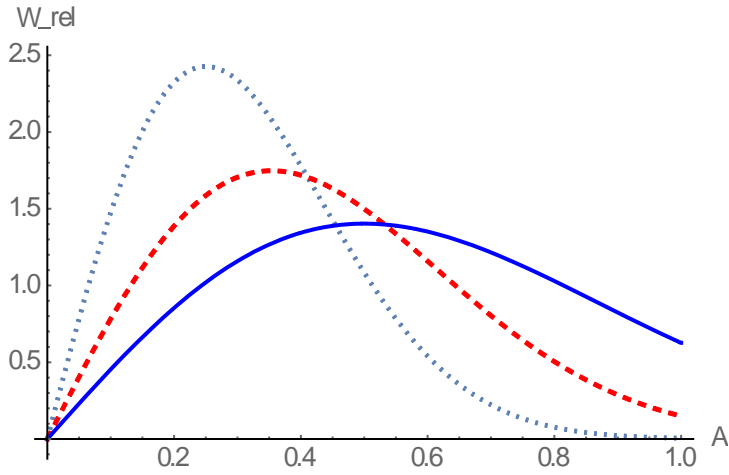
$$336 \quad W(y) = \int_y^{\infty} W_y^{\sin}(y; A) W_A(A) dA. \quad (5.4)$$

337 Formula (5.4) has an important practical meaning: by the measured distribution of the wave  
338 amplitudes far from the coast (re-computed on run-up amplitudes in the linear theory), it is possible  
339 to obtain the distribution of the wave run-up characteristics on the coast. The only requirement  
340 imposed on the wave ensemble is that it should not contain breaking waves, which should be  
341 somehow removed from the record. It immediately follows that the Gaussian field containing large  
342 amplitude tails does not fit this requirement, and it should be modified. Therefore, we assume the  
343 amplitude distribution to be finite for  $A < A_{max} = 1$ . **The narrow-band random wave field contains**  
344 **sine waves with almost constant frequency and random amplitude and phase. It means that if the**  
345 **wave amplitude is below the “breaking amplitude”  $A_{max} = 1$ , the breaking will not be implemented**  
346 **in any way, and the random wave run-up will take place without any breaking. Further calculations**  
347 **depend on the specific type of the amplitude distribution.**

348 Let us construct the finite amplitude distribution at which the linear field distribution is  
349 close to the Gaussian form and modify the Rayleigh distribution **for wave heights** in the area  
350  $A < A_{max} = 1$  (Fig. 5)

$$351 \quad W_A(A; A_{max}, A_s) = \frac{1}{1 - \exp(-2A_{max}^2 / A_s^2)} \frac{4A}{A_s^2} \exp\left(-2\frac{A^2}{A_s^2}\right), A \leq A_{max}, \quad (5.5)$$

352 to make the density function distribution normalized. Here,  $A_s$  is the so-called significant wave  
353 run-up height (an averaged value of 1/3 highest amplitudes). We would like to note here, that it  
354 follows from (2.11) and (2.12) that the extremal run-up characteristics in the nonlinear theory  
355 remain the same as in the linear theory. This means that the significant wave run-up height remains  
356 the same as in the nonlinear theory.



357

358

359 Fig. 5. The modified Rayleigh distribution (5.5) for different distribution values  $A_s/A_{max}$ ;  
 360 0.5 – the dotted curve, 0.7 – the dashed line, 1 – the solid line.

361

362 When  $A_s \ll A_{max} = 1$ , distribution (5.5) transforms into the Rayleigh one, which is  
 363 characteristic of the Gaussian initial distribution of a narrow-band random signal. With the help of  
 364 (5.5), it becomes possible to calculate the distribution function of shoreline oscillations for the  
 365 various wave energy. So, with the incident wave small amplitude ( $A_s \ll 1$ ), distribution (5.3) can  
 366 be replaced by a simpler expression (4.4) and the answer is the run-up distribution characteristics  
 367 in the linear theory:

$$368 \quad W_{lin}(y; A_{max}, A_s) = \frac{4}{\pi A_s^2 [1 - \exp(-2A_{max}^2 / A_s^2)]} \int_y^{A_{max}} \frac{A}{\sqrt{A^2 - y^2}} \exp\left(-2\frac{A^2}{A_s^2}\right) dA. \quad (5.6)$$

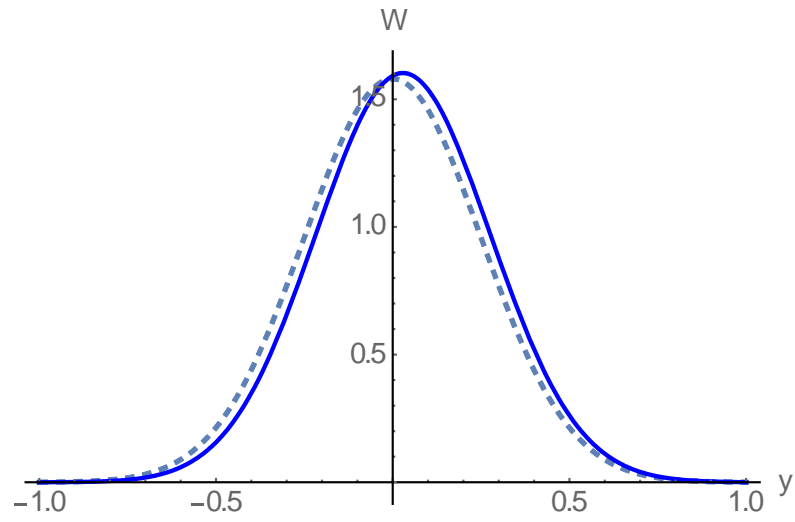
369 Besides, if  $A_s \ll A_{max} = 1$ , the integral (5.6) is reduced to the Gaussian distribution

$$370 \quad W_{lin}(y; A_s) = \frac{2}{\sqrt{2\pi} A_s} \exp\left(-2\frac{y^2}{A_s^2}\right), \quad (5.7)$$

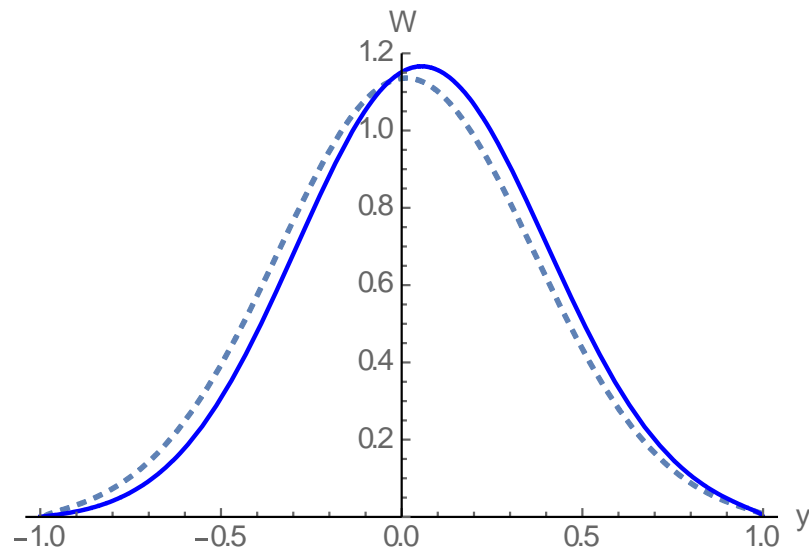
371 where,  $A_s = 2\sigma_y$ , and  $\sigma_y^2$  is the moving shoreline oscillation dispersion.

372 Fig. 6 shows the distribution of the run-up characteristics for different ratios of  $A_s/A_{max}$   
 373 values by formulas (5.4) and (5.5); they are shown in solid lines. Here the dashed lines show the  
 374 calculation results according to the linear theory (5.6). As one can see, with  $A_s/A_{max} = 0.5$  (the top  
 375 panel) and 0.7 (the middle panel), the linear distribution is close to the Gaussian one. Nonlinearity  
 376 leads to the asymmetry of the distribution function density in the direction of positive values  
 377 corresponding to the wave characteristics on the coast. If the undisturbed wave ensemble is made  
 378 of relatively large waves ( $A_s/A_{max} = 1$ ), their distribution is far from the Gaussian, both in the linear  
 379 and in the nonlinear approximation.

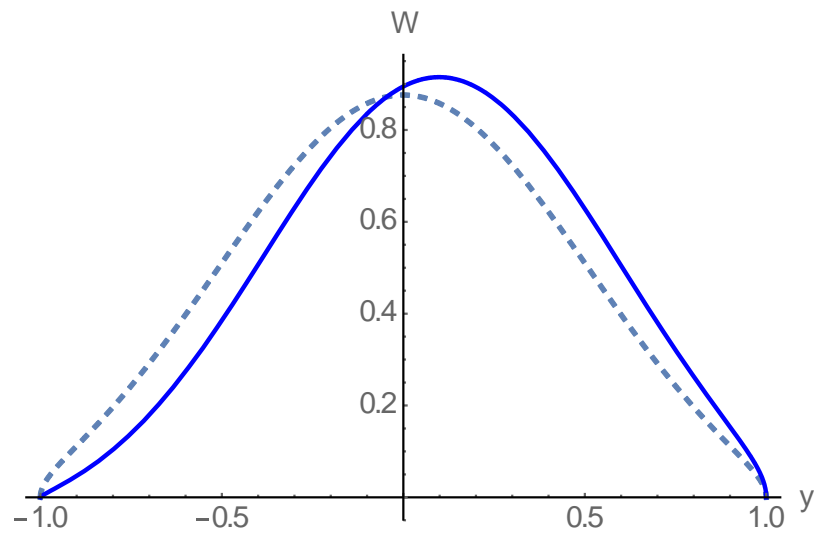
380



381



382



383

384

385

386

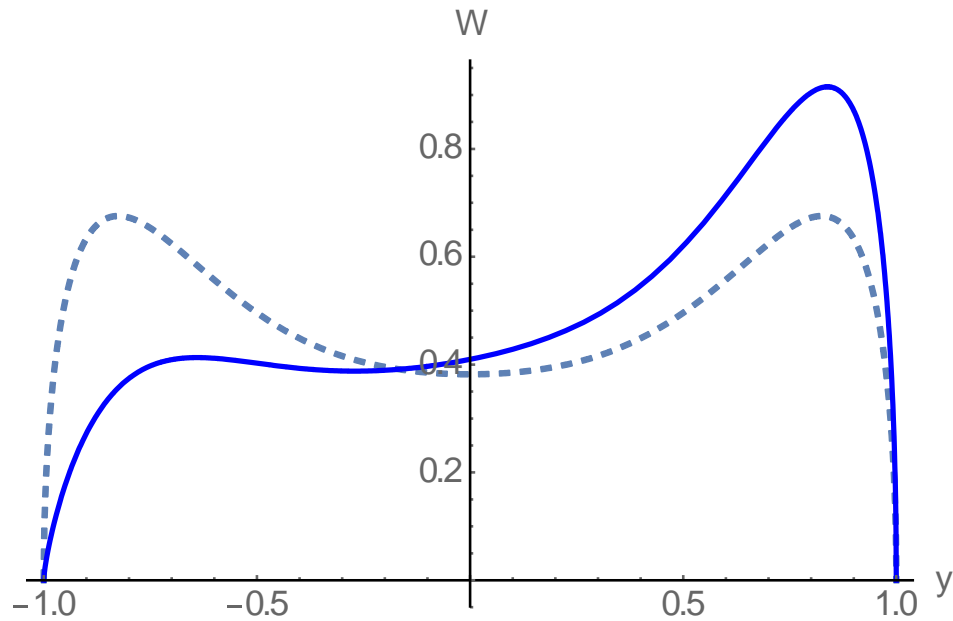
Fig. 6. The probabilistic density function of the vertical shoreline displacement in the nonlinear theory (solid lines) and in the linear theory (dashed lines) for different  $A_s/A_{max}$ : 0.5 values: (the upper panel), 0.7 (the middle panel) and 1 (the lower panel).



387 The finite ( $A < A_{max}$ ) power-law distribution concentrated mainly near the maximum  
 388 amplitude  $A_{max}$  can be considered as another example of undisturbed large-amplitude waves.

389 
$$W_A(A) = \frac{6A^5}{A_{max}^6}. \quad (5.8)$$

390 Fig. 7 shows the graphs of the probabilistic density function of the moving shoreline displacement  
 391 calculated by using formulas (5.4) and (4.4) in the linear theory and (5.3) in the nonlinear theory.  
 392 It is also seen in the figure that nonlinear effects lead to a strong asymmetry towards the positive  
 393 values, that is, to the wave amplification at the run-up up stage than at the run-down stage.



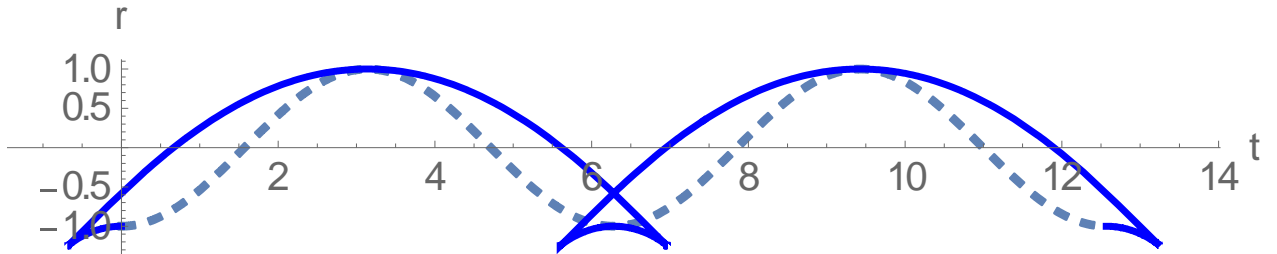
394  
 395 Fig. 7. Probabilistic density function of the shoreline vertical displacement in the linear  
 396 theory (the dashed line) and non-linear theory (the solid line)

397

### 398 6. The wave breaking effect on probabilistic run-up characteristics

399 The theory described above is valid for non-breaking waves. The mentioned wave ensemble,  
 400 strictly speaking, cannot be the Gaussian one, as it always has unlimited tails in the probability  
 401 density function. Let us briefly discuss what the formulas obtained for non-breaking waves lead  
 402 to in the presence of broken waves. Fig. 8 shows the parametric curve (3.11) - (3.12) when  $Br =$   
 403 2. Formally, the curve became multi-valued in the range of negative values corresponding to the  
 404 maximum water outflow from the coast. We have already indicated that the probability density  
 405 function of the moving shoreline vertical displacement  $W(\xi)$  coincides with the relative residence  
 406 time  $\xi(t)$  of the function in the interval  $(\xi, \xi + d\xi)$ , which is calculated by formula (3.1). In  
 407 contrast to negative cut-off bias values, in the area of positive values there is no ambiguity, and,

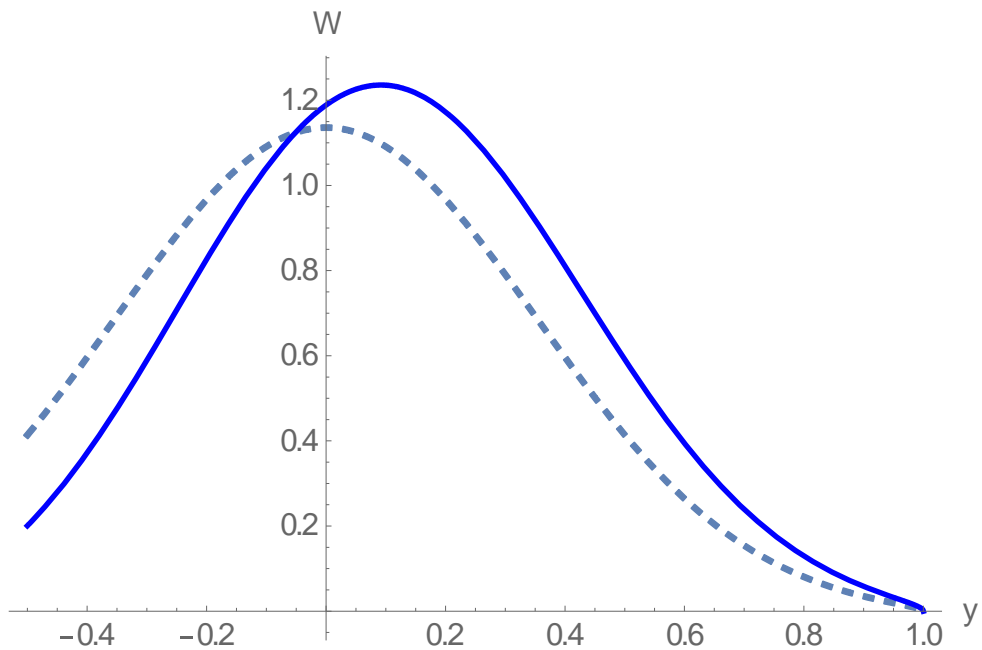
408 therefore, all the calculations can be carried out by using the formulas described above. An  
 409 example of such calculation with  $Br = 2$  and  $r > -0.5$  (in the zone of one-value solution) is shown  
 410 in Fig. 9. However, these results should be treated with caution. **If  $Br > 1$  the Jacobian breaks**  
 411 **down seawards of the shoreline. This may affect the probabilistic distribution on the positive side.**  
 412 This important issue requires going beyond the theory discussed in this article.



413  
414

415 Fig. 8. The parametric curve (3.11) - (3.12) with  $Br = 2$  (the solid curve) in comparison with the  
 416 linear problem with  $Br = 0$  (the dashed line)

417



418

419 Fig. 9. The probability density function at  $Br = 2$ , constructed by formulas (5.3), (5.4) and (5.5)  
 420 (the solid line) in comparison with the linear distribution (5.6) is the dotted line.  $A_s/A_{max} = 0.7$ .

421

## 422 7. Discussion and conclusion

423 In this paper, we study the run-up of irregular narrow-band waves with a random envelope  
 424 (swell, storm surges, and tsunami) on a beach of a constant slope. The work was carried out in the  
 425 framework of the nonlinear wave theory with one important assumption: there should be no

426 breaking waves in the wave ensemble. This restriction is quite strict for field and laboratory  
427 conditions, but nevertheless, there are cases when it is performed. For instance, 75% of historical  
428 tsunami waves climbed on the coast with no breaking (Mazova et al, 1983). In the experiments  
429 performed in the Warwick University tank and in the Large Tank in Hannover (Denissenko et al,  
430 2011, 2013), this condition was fulfilled.

431 The wave nonlinearity at the run-up stage leads to increased deviations from Gaussianity, as might  
432 be expected from general considerations. Nevertheless, it is shown that the probability distribution  
433 of the moving shoreline velocity does not depend on the wave nonlinearity and can be calculated  
434 within the linear theory framework. The same conclusion can be drawn about the distribution of  
435 the extreme run-up characteristics (the moving shoreline displacement and speed), which, in fact,  
436 has already been discussed earlier (Didenkulova et al, 2008). However, the probabilistic density  
437 function of the moving shoreline displacement differs from that predicted one in the linear theory  
438 framework. It is described by formula (5.4) by using either the theoretical or the measured  
439 distribution of the incident wave amplitudes. The paper gives the calculation results of the probable  
440 run-up characteristics with a modified Rayleigh distribution for wave amplitudes.

441 The wave breaking leads to the inapplicability of the wave run-up theory based on the  
442 Carrier-Greenspan transformation. If, nevertheless, the share of large amplitude waves is small,  
443 the breaking occurs mainly at the run-down stage, having little effect on the long-wave coast  
444 flooding characteristics (see Section 6). This question, however, requires a special study based on  
445 direct numerical solutions of the shallow-water equations or their nonlinear-dispersive  
446 generalizations.

447 Finally, it is worth noting that we considered the narrow-band wave run-up with a random  
448 amplitude and phase; as for the random waves with a wide spectrum – it is the problem of further  
449 consideration.

450 The obtained probability density functions of the vertical displacement of the moving  
451 shoreline are useful to compute statistical characteristics of flooding time and force on coasts and  
452 constructions, which are necessity for the mitigation of natural marine hazards.

453 **Now in practice various generalizations of shallow-water equations are used to analyze**  
454 **tsunami runup including wave dispersion, see for instance (Lovholt et al, 2012). Wave dispersion**  
455 **as a quadratic dissipative term that prevents us from getting analytical results, so their influence**  
456 **on statistical characteristics should be investigated in future.**

457

458 **Acknowledgment:**

459 The work is supported by the grants from the Russian Science Foundation: No.19-12-00256 (in  
460 part of computing the random Riemann wave characteristics) and No. 16-17-00041 (in part of  
461 computations the probability density function of the moving shoreline).

462

463 **References**

464

- 465 1. Anderson, D., Harris, M., Hartle, H., Nicolsky, D., Pelinovsky, E., Raz, A. and Rybkin, A.:  
466 Runup of long waves in piecewise sloping U-shaped bays, *Pure and Applied Geophysics*, 174,  
467 3185-3207, 2017.
- 468 2. Antuano, M. and Brocchini, M.: Maximum run-up, breaking conditions and dynamical forces  
469 in the swash zone: a boundary value approach, *Coastal Engineering*, 55, 732-730, 2008.
- 470 3. Antuano, M. and Brocchini, M.: Solving the nonlinear shallow-water equations in physical  
471 space, *J. Fluid Mech.*, 643, 207–232, 2010.
- 472 4. Aydin. B. and Kanoglu, U.: New analytical solution for nonlinear shallow water-wave  
473 equations, *Pure and Applied Geophysics*, 174, 3209–3218, 2017.
- 474 5. Bec, J. and Khanin, K.: Burgers turbulence, *Physics Reports*, 447, 1-66, 2007.
- 475 6. Burgers, J. M.: *The Nonlinear Diffusion Equation*. Dordrecht, D. Reidel, 1974.
- 476 7. Carrier, G.F.: *On-shelf tsunami generation and coastal propagation*. In *Tsunami: Progress in*  
477 *Prediction, Disaster Prevention and Warning*, eds. Tsuchiya, Y. & Shuto, N. Kluwer, Dordrecht,  
478 1-20, 1995.
- 479 8. Carrier, G.F. and Greenspan, H.P.: Water waves of finite amplitude on a sloping beach,  
480 *J. Fluid Mech.*, 4.97–109, 1958.
- 481 9. Carrier, G.F., Wu, T.T. and Yeh, H.: *Tsunami run-up and draw-down on a plane beach*, *Journal*  
482 *of Fluid Mechanics*, 475, 79-99, 2003.
- 483 10. Choi, J., Kwon, K.K. and Yoon, S.B.: Tsunami inundation simulation of a built-up area using  
484 equivalent resistance coefficient, *Coastal Engineering Journal*, 54, 1250015 (25 pages), 2012.
- 485 11. Dean, R.G. and Walton, T.L.: Wave setup. In: Kim, Y.C. (Ed.), *Handbook of Coastal and Ocean*  
486 *Engineering*. World Sci, Singapore, 2009.
- 487 12. Denissenko, P., Didenkulova, I., Pelinovsky, E. and Pearson J.: Influence of the nonlinearity  
488 on statistical characteristics of long wave runup, *Nonlinear Processes in Geophysics*, 18, 967-  
489 975, 2011.
- 490 13. Denissenko, P., Didenkulova, I., Rodin, A., Listak, M. and Pelinovsky E.: Experimental  
491 statistics of long wave runup on a plane beach, *Journal of Coastal Research*, 65, 195-200, 2013.

- 492 14.Didenkulova, I.: New trends in the analytical theory of long sea wave runup. In: Applied Wave  
493 Mathematics: Selected Topics in Solids, Fluids, and Mathematical Methods (Ed: E. Quak and  
494 T. Soomere). Springer, 265–296, 2009.
- 495 15.Didenkulova, I., Pelinovsky, E. and Sergeeva, A.: Runup of long irregular waves on plane  
496 beach. In: Extreme Ocean Waves (Eds: Pelinovsky E., Kharif C.), Springer, 83-94, 2008.
- 497 16.Didenkulova, I.I., Sergeeva, A.V., Pelinovsky, E.N. and Gurbatov, S.N.: Statistical estimates  
498 of characteristics of long wave run up on the shore, Izvestiya, Atmospheric and Oceanic  
499 Physics, 46, 530–532, 2010.
- 500 17.Didenkulova, I., Pelinovsky, E. and Sergeeva, A.: Statistical characteristics of long waves  
501 nearshore, Coastal Engineering, 58, 94-102, 2011.
- 502 18.Dobrokhotov, S.Yu.,Minenkov, D.S., Nazaikinskii, V.E. and Tirozzi, B.: Simple exact and  
503 asymptotic solutions of the 1D run-up problem over a slowly varying (quasiplanar) bottom. In  
504 Theory and Applications in Mathematical Physics, World Scientific, Singapore, 29-47, 2015.
- 505 19.Frisch, U.: Turbulence: the legacy of A. N. Kolmogorov, Cambridge University Press, 1995.
- 506 20.Frisch, U. and Bec, J.: Burgulence. In: New trends in turbulence (Eds: M. Lesieur, A.Yaglom  
507 and F. David), Springer EDP-Sciences, 341–383, 2001.
- 508 21.Gurbatov, S. N., Saichev, A. I. and Shandarin, S. F.: Large-scale structure of the Universe. The  
509 Zeldovich approximation and the adhesion model, Physics Uspekhi, 55, 223–249, 2012.
- 510 22.Gurbatov, S.N., Malakhov, A.N. and Saichev, A.I.: Nonlinear Random Waves and Turbulence  
511 in Nondispersive Media: Waves, Rays, Particles. Manchester University Press, 1991.
- 512 23.Gurbatov, S.N., Rudenko, O.V. and Saichev, A.I.: Waves and Structures in Nonlinear  
513 Nondispersive Media. Berlin, Heidelberg: Springer-Verlag, and Beijing: Higher Education  
514 Press, 2011.
- 515 24.Gurbatov, S.N. and Saichev, A.I.: Inertial nonlinearity and chaotic motion of particle fluxes,  
516 Chaos, 3, 333-358, 1993.
- 517 25.Gurbatov, S., Simdyankin, S., Aurell, E., Frisch, U. and Toth, G.: On the decay of Burgers  
518 turbulence, J. Fluid Mech., 344, 349-374, 1997.
- 519 26.Gurbatov, S.N., Deryabin, M.S., Kasyanov, D.A. and Kurin, V.V.: Evolution of narrow-band  
520 noise beams for large acoustic Reynolds numbers, Radiophysics and Quantum Electronics, 61,  
521 478–490, 2018.
- 522 27.Gurbatov, S., Deryabin, M., Kurin, V. and Kasyanov, D.: Evolution of intense narrowband  
523 noise beams, Journal of Sound and Vibration, 439, 208-218, 2019.

- 524 28.Harris, M.W., Nicolsky, D.J., Pelinovsky, E.N. and Rybkin A.V.: Runup of nonlinear long  
525 waves in trapezoidal bays: 1-D analytical theory and 2-D numerical computations, *Pure and*  
526 *Applied Geophysics*, 172, 885-899, 2015.
- 527 29.Harris, M.W., Nicolsky, D.J., Pelinovsky, E.N., Pender, J.M. and Rybkin, A.V.: Run-up of  
528 nonlinear long waves in U-shaped bays of finite length: Analytical theory and numerical  
529 computations, *J Ocean Engineering and Marine Energy*, 2, 113-127, 2016.
- 530 30.Hughes, M.G., Moseley, A.S. and Baldock, T.E.: Probability distributions for wave runup on  
531 beaches, *Coastal Engineering*, 57, 575-584, 2010.
- 532 31.Huntley, D.A., Guza, R.T. and Bowen, A.J.: A universal form for shoreline run-up spectra, *J.*  
533 *Geophys. Res.*, 82, 2577–2581, 1977.
- 534 32.Kaiser, G., Scheele, L., Kortenhaus, A., Lovholt, F., Romer, H. and Leschka, S.: The influence  
535 of land cover roughness on the results of high resolution tsunami inundation modeling, *Nat.*  
536 *Hazards Earth Syst. Sci.*, 11, 2521–2540, 2011.
- 537 33.Kendall, M.G. and Stuart, A.: *The Advanced Theory of Statistics. Volume I. Distribution*  
538 *Theory*. London. 1969.
- 539 34.Kian, R., Velioglu, D., Yalciner, A.C. and Zaytsev, A.: Effects of harbor shape on the induced  
540 sedimentation; L-type basin, *Journal of Marine Science and Engineering*, 4, 55-65, 2016.
- 541 35.Løvholt, F., Pedersen, G., Bazin, S., Kühn, D., Bredesen, R.E., and Harbitz, C.: *Stochastic*  
542 *analysis of tsunami runup due to heterogeneous coseismic slip and dispersion, J. Geophys. Res.*,  
543 *117, C03047, 2012. doi: 10.1029/2011JC007616.*
- 544 36.Macabuag, J., Rossetto, T., Ioannou, I., Suppasri, A., Sugawara, D., Adriano, B., Imamura, F.,  
545 Eames, I. and Koshimura, S.: A proposed methodology for deriving tsunami fragility functions  
546 for buildings using optimum intensity measures, *Nat Hazards*, 84, 1257–1285, 2016.
- 547 37.Madsen, P.A. and Fuhrman, D.R.: Run-up of tsunamis and long waves in terms of surf-  
548 similarity, *Coast. Eng.*, 55, 209–223, 2008.
- 549 38.Madsen, P. and Schaffer, H. A.: Analytical solutions for tsunami runup on a plane beach: single  
550 waves, N-waves and transient waves, *J. Fluid Mech.*, 645, 27-57, 2010.
- 551 39.Mazova, R.Kh., Pelinovsky, E.N. and Solov'yev, S.L.: Statistical data on the tsunami runup  
552 onto shore, *Oceanology*, 23, 698 – 702, 1983.
- 553 40.Molchanov, S.A., Surgailis, D. and Woyczynski, W.A.: Hyperbolic asymptotics in Burgers’  
554 turbulence and extremal processes, *Comm. Math. Phys.*, 168, 209-226, 1995.
- 555 41.Ozer, S.C., Yalciner, A.C. and Zaytsev, A.: Investigation of tsunami hydrodynamic parameters  
556 in inundation zones with different structural layouts, *Pure and Applied Geophysics*, 172, 931–  
557 952, 2015a.

- 558 42.Ozer, S.C., Yalciner, A.C., Zaytsev, A., Suppasri, A. and Imamura, F.: Investigation of  
559 hydrodynamic parameters and the effects of breakwaters during the 2011 Great East Japan  
560 Tsunami in Kamaishi Bay, *Pure and Applied Geophysics*, 172, 3473–3491, 2015b.
- 561 43.Park, H., Cox, D.T. and Barbosa, A.R.: Comparison of inundation depth and momentum flux  
562 based fragilities for probabilistic tsunami damage assessment and uncertainty analysis, *Coastal*  
563 *Eng.*, 122, 10–26, 2017.
- 564 44.Pelinovsky, E. and Mazova, R.: Exact analytical solutions of nonlinear problems of tsunami  
565 wave run-up on slopes with different profiles, *Nat. Hazards*, 6, 227–249, 1992.
- 566 45.Pelinovsky, D., Pelinovsky, E., Kartashova, E., Talipova, T. and Giniyatullin, A.: Universal  
567 power law for the energy spectrum of breaking Riemann waves, *JETP Letters*, 98, 237-241,  
568 2013.
- 569 46.Pedersen, G.: Fully nonlinear Boussinesq equations for long wave propagation and run-up in  
570 sloping channels with parabolic cross sections, *Natural Hazards*, 84, S599–S619, 2016.
- 571 47.Qi, Z.X, Eames, I. and Johnson E.R.: Force acting on a square cylinder fixed in a free-surface  
572 channel flow, *J Fluid Mech*, 756, 716–727, 2014.
- 573 48.Raz, A., Nicolsky, D., Rybkin, A. and Pelinovsky, E.: Long wave run-up in asymmetric bays  
574 and in fjords with two separate heads, *Journal of Geophysical Research – Oceanus*, 123, 2066-  
575 2080, 2018.
- 576 49.Rudenko, O.V. and Soluyan S.I.: *Nonlinear Acoustics*. Pergamon Press, NY, 1977.
- 577 50.Rybkin, A. Pelinovsky, E.N. and Didenkulova, I.: Nonlinear wave run-up in bays of arbitrary  
578 cross-section: generalization of the Carrier-Greenspan approach, *J Fluid Mechanics*, 748, 416-  
579 432, 2014.
- 580 51.Shimozono, T.: Long wave propagation and run-up in converging bays, *J. Fluid Mech.*, 798,  
581 457-484, 2016.
- 582 52.Synolakis, C.E.: The runup of solitary waves, *J. Fluid Mech.*, 185, 523–545, 1987.
- 583 53.Synolakis, C., Bernard, E.N., Titov, V.V., Kanoglu, U. and Gonzalez, F.I.: Validation and  
584 verification of tsunami numerical models, *Pure and Applied Geophysics*, 165, 2197-2228,  
585 2008.
- 586 54.Tinti, S. and Tonini, R.: Analytical evolution of tsunamis induced by near-shore earthquakes  
587 on a constant-slope ocean, *J. Fluid Mech.*, 535, 33–64, 2005.
- 588 55.Woyczynski, W.A.: *Burgers–KPZ Turbulence*. Gottingen Lectures, Berlin, Springer-Verlag,  
589 1998.

590 56.Xiong, Y., Liang, Q., Park, H., Cox, D. and Wang, G.: A deterministic approach for assessing  
591 tsunami-induced building damage through quantification of hydrodynamic forces, Coastal  
592 Engineering, 144, 1-14, 2019.  
593